


# A combined hydrological and hydraulic modelling approach for the flood hazard mapping of the Po river basin

Rita Nogherotto<sup>1,2</sup>  | Adriano Fantini<sup>1</sup> | Francesca Raffaele<sup>1</sup> |  
 Fabio Di Sante<sup>1,2</sup> | Francesco Dottori<sup>3</sup> | Erika Coppola<sup>1</sup> | Filippo Giorgi<sup>1</sup>

<sup>1</sup>International Centre for Theoretical Physics, Trieste, Italy

<sup>2</sup>Istituto Nazionale di Oceanografia e di Geofisica Sperimentale, Trieste, Italy

<sup>3</sup>European Commission, Joint Research Centre, Ispra, Italy

## Correspondence

Rita Nogherotto, International Centre for Theoretical Physics  
 Trieste, Italy.  
 Email: rnoghero@ictp.it

## Funding information

OGS and CINECA under HPC-TRES program, Grant/Award Number: 2020-12

## Abstract

The identification of flood prone areas is essential for a range of engineering, risk reduction and research applications. Here, we describe a combined hydrological and hydraulic modelling approach for the assessment of flood-prone areas and we present the results obtained over the Po river (Northern Italy). Runoff and river discharges are calculated through the hydrological model CHyM driven by GRIPHO, a new precipitation dataset for Italy. River flow data are used to obtain flood hydrographs for the CA2D hydraulic model, which calculates flood hazard maps at a resolution of 90 m. Flood simulations are run over a re-shaped HydroSHEDS digital elevation model that includes information of the channel geometry. Modeled flood hydrographs are compared with observed data for a choice of gauging stations, showing a good performance of the CHyM model. We validate the flood hazard maps against observed flood events and official hazard maps. For high return periods, modelled maps can correctly identify up to 67% of the flood extent, both on the Po River and on smaller tributaries, while performances are more variable for lower return periods. Overall, the proposed approach suggests a strong potential for further applications, such as flood hazard assessment under future climate scenarios.

## KEYWORDS

CA2D hydraulic model, CHyM hydrological model, flood hazard, flood mapping

## 1 | INTRODUCTION

The last few decades have seen increased interest towards the study of floods, their consequences on society and natural ecosystems and the development of measures to reduce their impact. Flood hazard maps are among the most important tools for flood risk management. According to the definition given by the European Floods

Directive (European Commission, 2007), flood hazard maps are designed to indicate the probability and/or magnitude of different flood scenarios over a given area and are used as a decision making tool for multiple purposes, ranging from infrastructure development to disaster response planning. Following the requirements of the Floods Directive, all the member states of the European Union have developed river flood hazard maps, using the

This is an open access article under the terms of the Creative Commons Attribution License, which permits use, distribution and reproduction in any medium, provided the original work is properly cited.

© 2021 The Authors. *Journal of Flood Risk Management* published by Chartered Institution of Water and Environmental Management and John Wiley & Sons Ltd.

approach deemed to be most appropriate. Italy is frequently affected by severe inundation events caused by inland water bodies (Istituto di Ricerca per la Protezione Idrologica and Consiglio Nazionale delle Ricerche, 2018), and this has led to the development of flood hazard maps already in the early 2000s under the responsibility of the local river basin authorities. The resulting national catalogue comprises flood maps developed with a considerable diversity of modelling approaches, data sets and coverage (ISPRA, 2017). In addition, the information on data and methods used is often difficult to retrieve and compare. As such, having a dataset at national scale developed with a uniform, consistent approach would allow a better comparison of flood hazard across different areas, thereby improving national-scale analyses.

Considerable portions of flood hazard maps in Italy were produced with one-dimensional hydraulic models (Autorità di bacino del fiume Po, 2012), mainly because of the limitations in topographic data and computational power. Today, two-dimensional (2D) models based on reduced complexity equations (i.e. where full flow equations are conveniently simplified; Bates, Horritt, & Fewtrell, 2010) can provide an adequate representation of flooding processes, generally outperforming one-dimensional models under a wide range of conditions (Castellarin, Domeneghetti, & Brath, 2011; di Baldassarre, Schumann, & Bates, 2009; Horritt & Bates, 2002). Moreover, due to huge advancements in parallel computing techniques, these models can be applied over large areas at high resolution, thus making simulations possible at continental and even global scale (Dottori et al., 2016; Sampson et al., 2015; Wing et al., 2017).

Nevertheless, models based on global datasets still have important drawbacks, such as the inability to accurately represent river bed geometry due to the lack of global channel bathymetry data (Yamazaki et al., 2019). Such limitations can be overtaken when focusing on data-rich areas, however, recent scientific studies on flood hazard estimation in Italy have mostly focused on examining specific limited areas of interest (Di Salvo, Ciotoli, Pennica, & Cavinato, 2017; Marchesini et al., 2016; Morelli, Battistini, & Catani, 2014; Sole, Giosa, Nol'e, Medina, & Bateman, 2008), particular past events (Amadio, Mysiak, Pecora, & Agnetti, 2013; Marchi, Borga, Preciso, & Gaume, 2010; Masoero, Claps, Asselman, Mosselman, & Di Baldassarre, 2013; Norbiato, Borga, Sangati, & Zanon, 2007; Santo, Di Crescenzo, Del Prete, & Di Iorio, 2012) or flood risk rather than hazard (Albano, Mancusi, & Abbate, 2017; Salvati, Bianchi, Rossi, & Guzzetti, 2010). In this study, we describe a combined hydrological and hydraulic modelling approach which uses the Cetemps Hydrological Model (CHyM,

Coppola, Tomassetti, Mariotti, Verdecchia, and Visconti (2007)) and a modified version of the CA2D hydraulic model (Dottori & Todini, 2011), hereafter referred to as CA2D<sub>par</sub>. The use of a combined hydrological and hydraulic approach to calculate discharge (Bárdossy, 2007; Khan et al., 2011) has considerable advantages, such as the applicability over ungauged regions and the possibility of assessing the impact of changes in climate and/or land cover on floods. While such modelling approach has been applied in previous works to map flood hazard at the European scale (Alfieri et al., 2014; Dottori, Alfieri, Bianchi, Skoien, & Salamon, 2021), here we use different data and models with some relevant advances. First, our modified CA2D<sub>par</sub> has been upgraded to use a parallel algorithm which allows the model to be run on multiple processors, thus increasing considerably its computational efficiency. Furthermore, to better represent river flow and flooding processes, we produced a re-shaped digital elevation model including information of river channels, which is obtained by adjusting channel bed elevation in a way that discharges associated to return periods of 1.5 years produce no floods, as they represent the conveyance capacity of the river channel. The method we describe aims at finding a general way to account for river channel geometry also in regions where there is no available information on river natural banks. Finally, the modelling framework takes advantage of national meteorological datasets which provide accurate input data for hydrological and flood simulations. In particular, the use of these datasets allows simulating flood extent on minor rivers, which were not included in previous continental maps.

The proposed methodology has been applied over the entire Italian territory, however, for illustrative purposes, here we focus on the results obtained over the Po river basin. The Po River exhibits the largest average daily discharge in the Italian peninsula, and 40% of the gross domestic product of Italy is produced in its river basin (Montanari, 2012). The Po River Basin Authority (AdbPo, [www.adbpo.gov.it](http://www.adbpo.gov.it)) provides flood hazard maps for the entire Po basin for three return periods (20–50, 100–200 and 500 years). These are relatively well documented and available for use (Autorità di bacino del fiume Po, 2012), thus providing a valuable benchmark for our modelling procedure. In Section 2, we describe the observational and simulation data along with the method applied for flood hazard assessment over the western basin of the river Po. Section 3 presents the results, including the validation of the flood hydrographs and the simulated flood hazard maps, hereafter referred to as 'ICTP2H' maps, against observations and other existing maps.

## 2 | DATA AND METHODS

The approach proposed here assumes that flood hazard maps over a large domain can be derived from an ensemble of small sub-simulations of flood processes arranged to cover the entire river network (Alfieri et al., 2013, 2014; Dottori, Salamon, et al., 2016). The procedure is composed of the following steps: (1) hydrological simulations are setup and calibrated for the production of long-term discharge time series; (2) flood hydrographs are derived for different selected return periods; (3) floodplain hydraulic simulations are performed and the flood maps for each return period are produced. These three steps, illustrated in Figure 1 are described in the following subsections.

### 2.1 | The observation data and the hydrological model CHyM

Hydrological simulations are performed using the CETEMPS Hydrological Model (CHyM) (Coppola et al., 2007), a distributed hydrological model developed by the Centre of Excellence at the University of L'Aquila. CHyM uses information from a Digital Elevation Model

(DEM) and employs an eight flow direction (D8) approach (Jenson & Domingue, 1988; Martz & Garbrecht, 1992; Tribe, 1992), using cellular automata algorithms to resolve local singularities and no-flow points (Coppola et al., 2007). Input precipitation from various sources can be assimilated, including gridded precipitation from observations and models. Discharge is routed through each grid cell using continuity and momentum equations based on the kinematic shallow water approximation of Lighthill and Whitham (1955). Potential evapotranspiration is computed as a function of the reference evapotranspiration, that is the evapotranspiration in saturated soil conditions. For details about the computation of the reference evapotranspiration we refer to Todini (1996) and Thornthwaite et al. (Thornthwaite & Mather, 1957).

CHyM is specifically designed for Italian river catchments and has been widely tested for a variety of regions across Italy, and in particular for the Po basin (Coppola et al., 2014; Tomassetti, Coppola, Verdecchia, & Visconti, 2005a; Verdecchia, Coppola, Tomassetti, & Visconti, 2009), the largest of the peninsula. The domain chosen for this study consists of the upper part of this catchment, and matches one of the nine operational domains simulated by CETEMPS to forecast potential

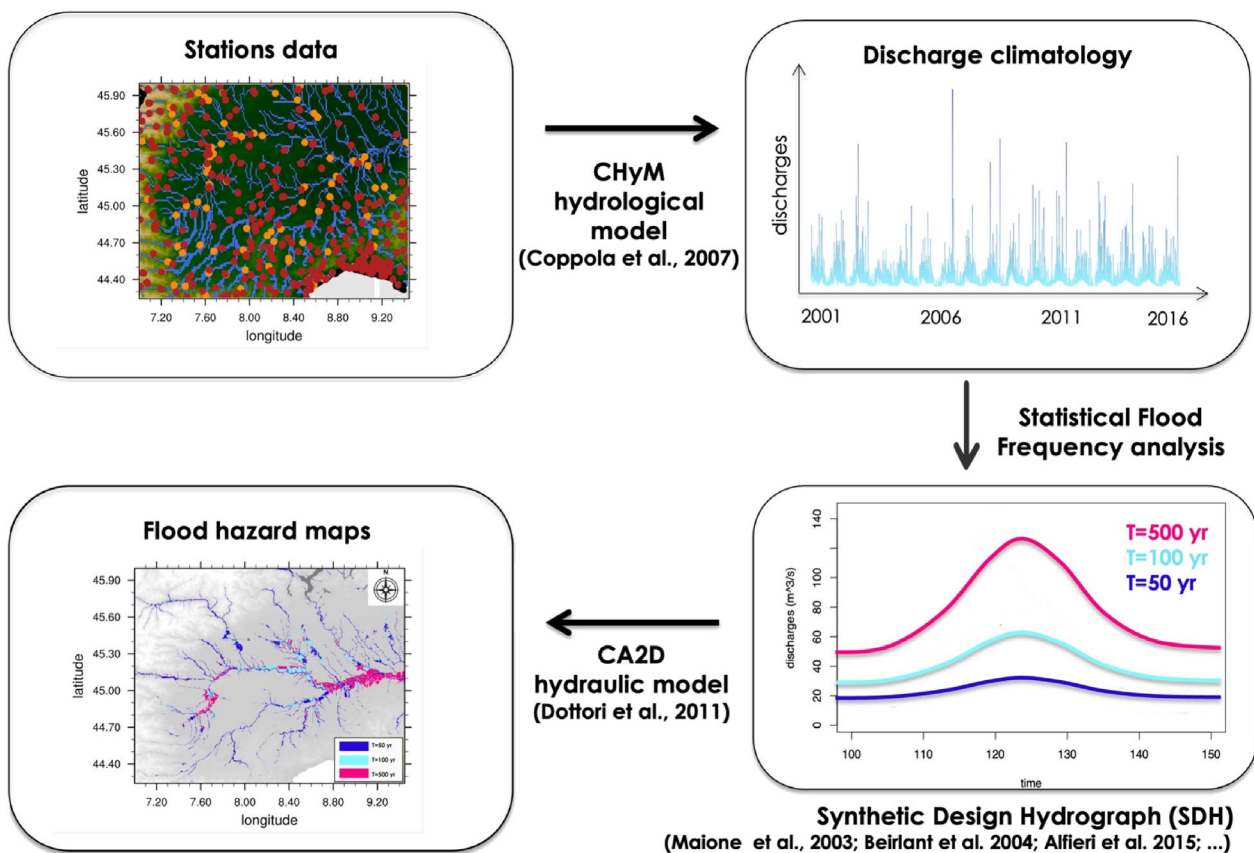


FIGURE 1 Schematic view of the approach used in this study

floods over the Italian territory using stress indices (Tomassetti, Coppola, Verdecchia, & Visconti, 2005a; Verdecchia et al., 2008). The simulations performed for this study are part of a study (Fantini, 2019) focused on the impact of climate change on flood hazard for the Italian territory. The calibration of the model is based on previous studies (Coppola et al., 2014; Tomassetti et al., 2005a; Verdecchia et al., 2009). In particular, the model output is calibrated against observed discharge stations available along the river path with the model forced using observed precipitation and temperature over a 10 years period for which the observations are available (2001–2010). The evapotranspiration and the return flow parameters are calibrated to implicitly take into account the loss of water due to human activities, whereas the infiltration parameters are calibrated to account for the soil characteristics. The performance of the hydrological model was evaluated using two different datasets of river discharge observations: a daily discharge datasets from the standard European Water Archive (EWA, 2014) and three hourly discharge datasets provided by CETEMPS. Due to the poor station availability the validation was performed only over two CHyM domains, one covering the largest Italian river basin (the Po river) and the other over central Italy (including the second largest river basin in Italy, the Tevere). The used metrics showed good agreement with observations for most of the stations covered by the two domains except for the northernmost stations of the Po domain and the easternmost stations of the Central Italy domain. The index of agreement is found  $>0.6$  for most of the stations over Po and Tevere basins. Similar results are shown using other metrics as the Kling-Gupta efficiency and the Pearson correlation coefficient. The model is able to reproduce the whole range of discharge events, though with a slight overestimation of high flow discharge events and frequency of low flow discharge events. In general, as expected, the model tends to show better performances in simulating larger basins.

A spatial resolution of 900 m, a spin-up time of 6 months and a timestep of 1.2 min for the solution of the prognostic continuity equation are employed. Testing with higher spatial and temporal resolutions did not result in an improved representation of river discharges when compared with observed data (Fantini, 2019). The choice of the DEM is crucial to ensure a correct river routing, especially in large, flat areas such as the Po plain. Our simulations are based on the HydroSHEDS DEM (Lehner, Verdin, & Jarvis, 2013), which is specifically conditioned for use in hydrology applications and offers very high resolution (around 90 m). The simulations span the period 2001–2016 and are driven by the newly developed hourly precipitation dataset GRIPHO (Fantini, 2019; Fantini, Di Sante, Coppola, Verdecchia, &

Giuliani, 2021), which includes quality-controlled data from 3712 precipitation stations covering the Italian territory interpolated on a 12 km resolution grid. MM5 weather forecasts (Grell et al., Grell, Dudhia, & Stauffer, 1994) operationally in use at CETEMPS for more than 20 years (see e.g. Bianco et al., 2006) are employed to fill data gaps in GRIPHO. Further information on the hydrological simulations used for this study, including validation against discharge observations, can be found in Fantini (2019).

## 2.2 | Processing the hydrological inputs: The flood hydrographs

The procedure applied here to construct flood hydrographs is based on the work of Maione, Mignosa, and Tomirotti (2003), who performed a Flood Frequency Analysis for the Po river basin. We thus refer to that paper and to Fantini (2019) for a detailed description of it. For each river segment the main quantity relevant for the estimation of the flood extent is the maximum discharge that can lead to flood. A way to estimate a feasible range of values for this quantity is a statistical-probabilistic analysis on the basis of observed (or modelled) data to derive the frequency of occurrences. The aim of this analysis is the determination of the relationship between discharge and return period of flooding by constructing a flood hydrograph ( $H_f$ ), as done in Maione et al. (2003). We used a simulated discharge time series to collect the annual maximum discharges, which are then statistically fitted to an extreme value distribution (here the Gumbel distribution) to be able to extend the simulation of extreme events to any return period. When performing the analysis for each historical flood peak, the centre of the duration window of width  $D$  is chosen to maximize the average computed discharge  $Q_D$ :

$$Q_D = \frac{1}{D} \max \int_t^{t+D} Q(T) dT, \quad (1)$$

where  $t$  and  $\tau$  represent time. These curves, called Flow Duration Frequency reduction curve (FDF) represent the typical discharge for each value of the return period  $RP$  averaged over any duration  $D$  ranging from 0 (the instantaneous discharge, for which FDF represents the peak flood discharge) to a value  $D$  large enough for the basin. Since we hypothesized the Gumbel distribution as statistical distribution of the annual maximum discharges, the equation for the explicit calculation of the FDF curves is:

$$Q_D(R_P) = u - \alpha \ln \left[ -\ln \left( 1 - \frac{1}{R_P} \right) \right] \quad (2)$$



where the parameters  $u$  and  $\alpha$  are estimated from the fit, by applying the maximum likelihood method. A Flow Duration Frequency reduction curve is therefore computed at each grid point in the river network. The flood hydrographs  $H_f$  are then calculated by imposing that the maximum average discharge for each duration coincides with the value obtained from the FDF curves in a given duration  $D$  for each value of the  $R_p$ . The shape of the final design synthetic hydrograph is determined by the peak-duration ratio  $r_D$ , that is the ratio of the time before the peak and the total duration  $D$  of the averaging window. An example of data sampling of  $Q_D$  and  $r_D$  from historical hydrographs is presented in figure 1 of Maione et al. (2003). We assume symmetry of the hydrograph, meaning that the flood peak is always in the centre of the two hydrograph limbs, which is a valid assumption for medium large catchments as done in Alfieri et al. (2014).

These curves allow us to calculate a typical flood event discharge time series for any location and return period, starting only from the time series of yearly maximum discharges. Once the  $H_f$  are estimated, they are used as input data for the hydraulic model in order to calculate the corresponding maximum flood inundation extent and depth (see Section 2.3). As an example application of this procedure, Figure 2 shows  $H_f$  for seven

return periods using data from the Farigliano station on the Tanaro river in the South-Western part of the study area, whose data are taken from the European Water Archive (EWA, 2014).

### 2.3 | Modelling the flood inundation: The hydraulic model

Floodplain hydraulic simulations are performed using a modified version of the 2D hydraulic model CA2D originally developed by Dottori and Todini (2011). We use as starting point the model version proposed by Dottori, Salamon, et al. (2016), which adopts a raster computation grid with an 8-direction link network (Moore neighbourhood rule, Parsons and Fonstad (2007)) and the semi-inertial formulation of the momentum equation (Bates et al. (2010)). Note that the model uses the same flow equations for both the channel flow and floodplain flow. In this new version, hereafter referred to as  $CA2D_{par}$ , the physics is unchanged with respect to the original version but the code is translated into a more recent fortran standard (Fortran90) and is parallelized using the message passing interface (MPI) communication.

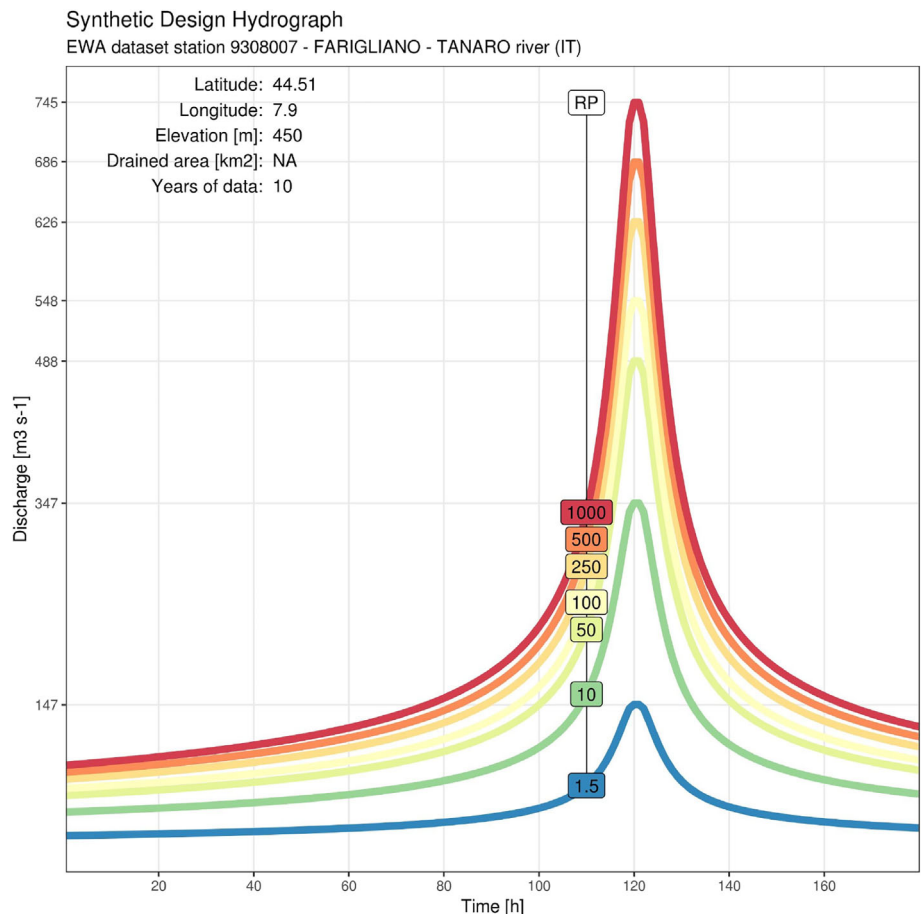


FIGURE 2 Example flood hydrographs computed following the procedure described in Section 2.2 for a station on the Tanaro River, tributary of the Po river. Seven return periods (1.5, 10, 50, 100, 250, 500, and 1000 years) are shown

To evaluate the performance and scalability of the model, a set of 11 different simulations were carried out and the wall clock times in seconds as a function of number of cores are reported in Figure 3. The domain used for the scalability tests has a spatial extension of 0.3 by 0.3° with a resolution of 90 m, and the tests were run on the ICTP HPC cluster (Argo <http://argo.ictp.it/>) with 36 nodes each having 12 Sandybridge Cores and 32 GB per node. The parallelization of the code increases the performance of the model by a factor of up to 7.5 times with respect to the original model, even with a limited number of cores. The speed increases with the number of cores up to 60 cores, when the best performance is reached (Figure 3).

## 2.4 | The production of the ICTP2H flood maps

### 2.4.1 | The digital elevation model

Currently, the Shuttle Radar Topography Mission (SRTM) DEM (Farr et al., 2007; Rabus, Eineder, Roth, & Bamler, 2003) is considered as one of the best openly available datasets for flood modelling with near-global coverage (Hirt, Filmer, & Featherstone, 2010; Jing, Shortridge, Lin, & Wu, 2014). The void-filled HydroSHEDS variant of SRTM was used in this work with 3 arc sec resolution (Lehner, Verdin, & Jarvis, 2006, 2008).

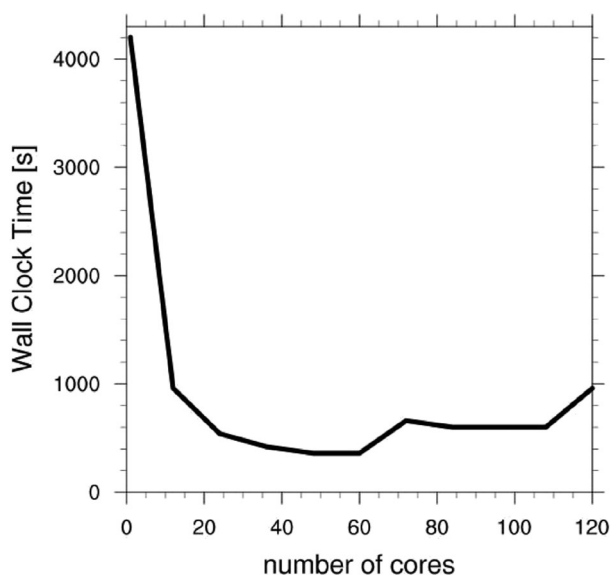


FIGURE 3 Wall-clock time (s) variation with the number of cores achieved with the parallelization of the CA2D model

### 2.4.2 | The ‘digging method’

As described in Neal, Schumann, and Bates (2012) and Sampson et al. (2015), representing river channels in simulations is necessary to guarantee acceptable results in terms of flood depths and extent. While river channel widths can be estimated remotely at near-global scale (Yamazaki et al., 2014), direct or indirect measures of channel bathymetry are not yet available, and channel geometry is usually estimated with empirical hydraulic geometry functions (Andreadis, Schumann, & Pavelsky, 2013; Sampson et al., 2015). Natural and artificial river defenses are also challenging to incorporate in large-scale models, as they are not detected by global DEMs (Dottori, Salamon, et al., 2016). Moreover, ground-based information on river flood defenses generally refers only to limited areas (e.g. Brandimarte & Di Baldassarre, 2012; Te Linde, Bubeck, Dekkers, De Moel, & Aerts, 2011), therefore continental and global datasets have to rely on modelled data (Scussolini et al., 2016).

In order to estimate the channel conveyance, here we use the near-global database of bankfull depths, based on hydraulic geometry equations and the HydroSHEDS hydrography dataset described in Andreadis et al. (2013). The novel idea is to link the channel geometry to the discharge return period, as it guarantees that channels, properly sized, are able to contain the simulated flows. The method also mitigates the problem of missing information on the geometry of the river we use the bankfull depths to artificially ‘dig’ the HydroSHEDS DEM. We assign to each river segment of depth  $d_o$  given by Andreadis et al. (2013) a new depth  $d_n$  proportional to the estimated depth  $d_o$  according to:

$$d_n = kd_o \quad (3)$$

where  $k$  is the digging coefficient parameter, spatially uniform along the river and its tributaries. This coefficient is chosen considering that the 1.5 year return period is assumed as the conveyance capacity of the river channel (Andreadis et al., 2013; Harman, Stewardson, & DeRose, 2008; Leopold, 1994; Neal et al., 2012; Sampson et al., 2015), that is the 1.5 year return period corresponds to zero flooded areas. This new depth is then subtracted from the HydroSHEDS DEM. It is important to note that digging the channel is applied to include the river bed permanently covered by water, which is not represented in the DEM, and that no assumptions are made for the rivers’ widths. It is not meant to mimic the effect of flood protection structures, such as river dykes, which requires a separate treatment. Indeed, where floodplains are protected by a dyke system, overflowing may be allowed

in a limited portion of floodplain between the river bed and the main river dykes in order to reduce flood peaks. For instance this is what happens along the main stem of the Po River (Castellarin et al., 2011), as described in Section 3.3. Therefore, representing dykes would require to ‘raise’ DEM pixels corresponding to river banks in order to reproduce the blockage effect (as done by Wing et al., 2017). Such approach could be done over the Po River where the level of flood protection is known, but this is not the case for the majority of river basins in Italy and Europe. Given that our goal is to develop a methodology applicable everywhere, we opted to not use local information for the model setup.

### 2.4.3 | The ‘virtual stations’ and flood simulations

As stated in Section 2.1, a 15-year continuous discharge time series covering the Italian territory is generated using the CHyM hydrological model from January 2001 to December 2016. Flood peaks with 50, 100, 500 year return periods are derived for each river point in the model and downscaled to the river network at 3 arc sec resolution. Flood hydrographs are then used to perform small scale floodplain hydraulic simulations on points which will be hereafter referred to as ‘virtual stations’. These are located every 10 km along the river network for rivers with drainage areas larger than  $A = 5 \text{ km}^2$  using the hydraulic model CA2D<sub>par</sub> (see red dots in Figure 4). For each virtual station the simulation is run over a sub-domain of  $0.3^\circ \times 0.3^\circ$  size ( $\sim 30 \times 30 \text{ km}$  at this latitude), chosen to optimize the computational efficiency, as the simulation time is strongly affected by the size of the domain.

Due to the relatively small size of each simulated sub-domain, the duration of all flood simulations was set to 240 h, a value based on the maximum time of

concentration over the Po River (Alfieri et al., 2014), which allows us to reproduce flood wave dynamics throughout the entire river network. For each return period, a total of 474 simulations were performed and merged to produce a Western Po river flood hazard map, taking the maximum depth value where more maps overlap. In each computation domain, Manning’s roughness values for the hydraulic simulations are derived from the Corine Land Cover map (Copernicus Land Monitoring Service, 2020). Note that we did not perform a specific calibration of roughness values, but we used values taken from previous studies (Alfieri et al., 2014; Alfieri, Burek, Feyen, & Forzieri, 2015) that applied similar 2D model codes over comparable grid resolutions. The range of values goes from  $0.2 \text{ m}^{1/3} \text{ s}$  for forest areas to  $0.04 \text{ m}^{1/3} \text{ s}$  for river channels, following Alfieri et al. (2015).

In all the simulations a free flow boundary condition is assumed at the edge of the domain, while the initial water level for the sea and internal water bodies is given by the local DEM value. We do not include levees in the model domain, as the information on their geometry is not available from remotely sensed datasets, therefore we assume that overflow occurs when channel conveyance is exceeded. The flood maps for the Western Po obtained for return periods of 50, 100 and 500 years are shown in Figure 5, where smaller return period floods are overlaid to larger ones.

## 2.5 | Maps validation

Validation of flood hazard models is achieved through the evaluation of the model accuracy in estimating the probability of flood occurrence and of relevant hazard variables of the flood event (e.g. flood extent and depth, flow velocity). Unfortunately the evaluation is strongly limited by the scarce availability of reference flood maps and flood observations, and is a key topic in flood risk

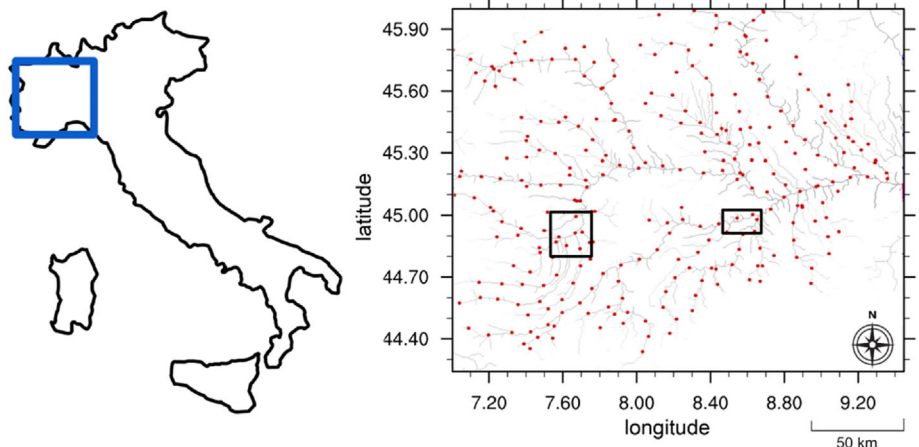


**FIGURE 4** Virtual stations selected for drainage areas larger than  $A = 5 \text{ km}^2$  and regularly spaced every 10 km along the high-resolution river network of the analysed domain (blue box on the left). Black square boxes show the flooded area analysed in Section 3.2

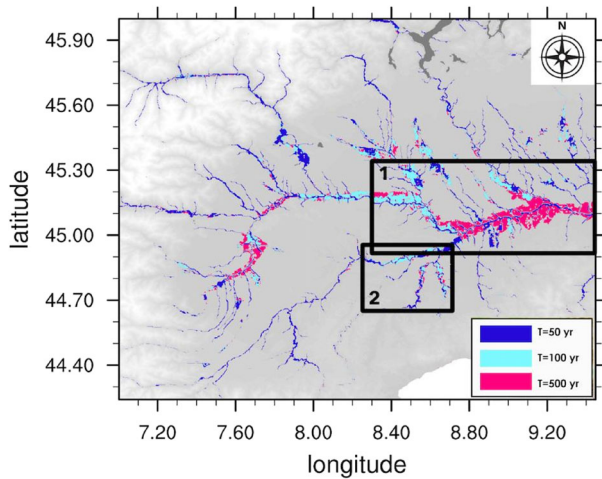


**FIGURE 5** Western Po river flood hazard map for the return periods of 500, 100, and 50 years obtained using the CHyM hydrological model and the CA2D<sub>par</sub> hydraulic model combined. The black boxes indicate the areas analysed for comparison in Section 3.3

analysis. Various methods were suggested by previous studies. One consists in comparing the simulated maps with other reference maps based on the statistical estimation of peak discharges (Pappenberger, Dutra, Wetterhall, & Cloke, 2012); another method consists of comparing the simulated flood event maps against observations of flood extent for events of comparable magnitude, using satellite flood images, aerial surveys or ground surveys (Rudari et al., 2015). A further approach consists of comparing the simulated flood maps against reference hazard maps prepared by national or local authorities (Alfieri et al., 2014).

The validation of simulated ICTP2H flood maps against observations (Section 3.2), and against reference maps (Section 3.3) is performed using indices proposed in the literature (Alfieri et al., 2014; Bates & de Roo, 2000; Dottori, Salamon, et al., 2016). The Hit Ratio index ( $H_R$ ), defined as:

$$H_R = (F_m \cap F_o) / (F_o) \quad (4)$$

measures the agreement of ICTP2H flood maps ( $F_m$ ) with existing maps ( $F_o$ ). This index does not take into account the overprediction or underprediction of the flooded area, therefore two other measures are calculated to account for this: the False Alarm index ( $F_A$ ), defined as:

$$F_A = [F_m - (F_m \cap F_o)] / (F_o) \quad (5)$$

where  $F_m - (F_m \cap F_o)$  is the flooded area wrongly predicted by the model, and the Critical Success index ( $C_S$ ), defined as:

$$C_S = (F_m \cap F_o) / (F_m \cup F_o). \quad (6)$$

### 3 | RESULTS AND DISCUSSION

The method was tested over the upper Po basin due to previous experience with the hydrological model in this domain (Coppola et al., 2014) and the availability of reliable observed discharge data (Fantini, 2019). Results are organized as follows: first, we compare the flood hydrographs reproduced by the hydrological model with those obtained using observational data (Section 3.1); then, we evaluate the simulated flood extent maps against observations for two case studies of real flood events (Section 3.2) and against official flood maps produced by the River Po Authority (Adbpo) along with simulated pan-European maps produced by the Joint Research Center's (JRC) for return periods of 50, 100 and 500 years (Section 3.3).

#### 3.1 | Validation of the flood hydrographs

The flood hydrographs  $H_f$  were first produced using observations from 31 gauge stations along the Po river provided by CETEMPS, covering on average a period of 15 years, and then compared with those obtained using the CHyM model at the same stations. Figure 6 shows the results of the comparison. The  $H_f$  are generally closely reproduced by the model, both in terms of peaks (Figure 6a) and flood volume (Figure 6b) with slightly higher biases for the low values of flood peaks and volume. The coefficient of determination ( $R^2$ ) between observed and simulated data averaged over all the station and the return periods is 0.85 for the  $H_f$  volumes and 0.92 for the  $H_f$  peaks, which are similar values to those reported in Rojas, Feyen, Dosio, and Bavera (2011) for a hydrological model for Europe without bias correction of climate data and in Paprotny and Morales-Nápoles (2017).

#### 3.2 | Comparison against observations: Two case studies

In order to provide the evaluation of our flood hazard mapping methodology we consider two case studies of real flood events occurred in Northern Italy: the first event took place along the Tanaro river, a Po tributary, in November 1994, while the second event occurred along the Po river in November 2016. The November 1994 flood hit the Italian provinces of Cuneo, Torino and Alessandria causing 70 deaths and the displacement of 2.226



people. According to the regional Arpa agency the discharge recorded during the event may have reached a return period of 'more than 100 years' (Arpa Piemonte). November 2016 was characterized by a heavy rainfall event involving the territory of North west Italy, in particular the Regions of Piemonte and Liguria. The bad weather conditions and the persistence of intense precipitation caused the increase of hydrometric levels of all the rivers in these regions, and in particular in the Po river basin. Figure 7a,b show in green the flooded area for a  $20 \times 13$  km region south of Alessandria and a  $36 \times 20$  km area south of Turin along the Po and the

Tanaro rivers (the areas are indicated with the black squares in Figure 4). The images are provided by aerial photographs taken by the Arpa Piemonte region for the event shown in panel (a). The observed flood in panel (b) was detected by the satellite COSMO-SkyMed (CSK) (Covello et al., 2010), a four-satellite constellation which gives the possibility of acquiring X-band Synthetic Aperture Radar (SAR) data during day and night, regardless of weather conditions. It provides radar data characterized by short revisit time and therefore useful for flood mapping evaluation, however with the well-known limitations due to the specular reflection and the double

**FIGURE 6** Comparison of simulated (CHyM) and observed (Obs)  $H_f$  volume (a) and discharges peaks (b) for 31 gauge stations along the Po river, for three return periods

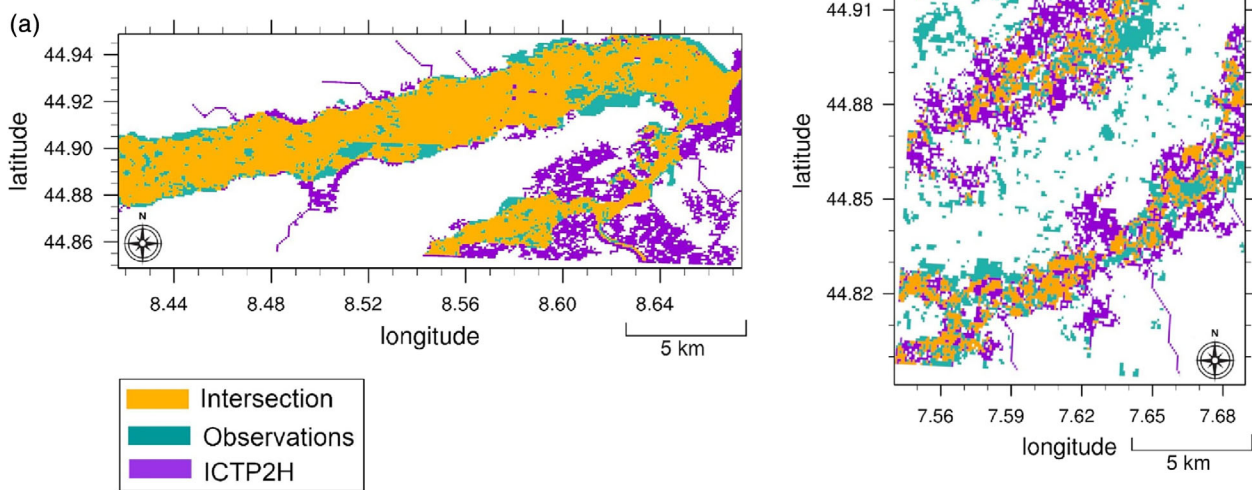
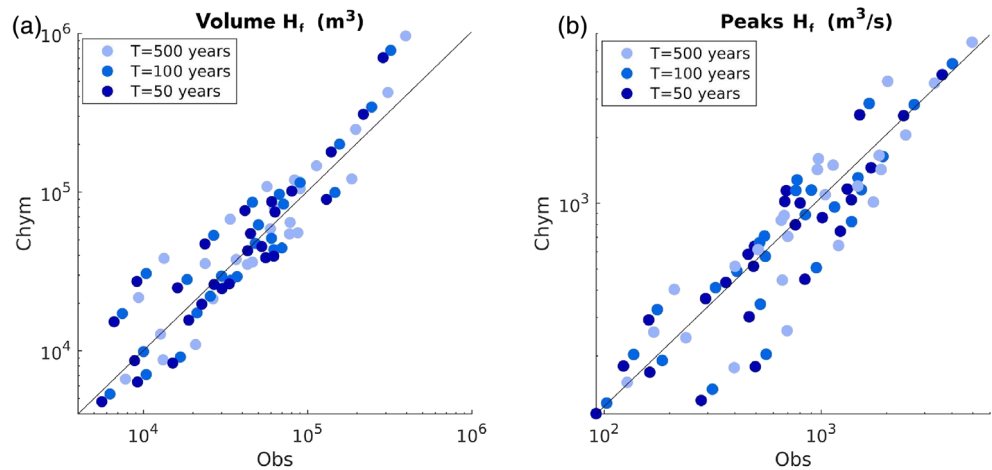


**FIGURE 7** Case studies used for the validation of the method: (a) shows the flood occurred in November 1994 in the region of Piemonte acquired by the Piemonte region through aerial photography, compared with the flood as modelled by the combined CHyM-CA2D<sub>par</sub> method associated to a return period of 100 yr, (b) shows the flood of November 2016 in the south of Turin acquired by the satellite COSMO-SkyMed (COSMO-SkyMed image ©ASI [2016]. All rights reserved) compared with the flood associated to a return period of 100 yr as modelled by the combined CHyM-CA2D<sub>par</sub> method

bounce backscattering (Balz & Stilla, 2009; Pulvirenti, Pierdicca, & Chini, 2010).

In violet, we show the ICTP2H flood maps corresponding to a return period of 100 years while in orange the intersection between simulated and observed floods. Table 1 shows the performance indices (Equations 4–6) calculated for the ICTP2H flood ( $F_m$ ) against the observed ones ( $F_o$ ). We can see that the model reproduces fairly well the event occurred on the tributary of the Po river, the Tanaro river, shown in Figure 7a with a Hit Rate of 0.82 and a False alarm of 0.31. According to available reports, in this area the embankments were overflowed or broke at different locations, implying that the floodplain was almost entirely flooded (Arpa Piemonte). As such, the flood extent in Figure 7a is likely shaped by the morphology of the river floodplains, rather than by embankments.

Indices indicate lower skills for the event in Figure 7b, with a lower hit rate and a high ratio of false alarms. This result can be attributed to the low quality of SRTM elevations in this area, which produces checkerboard patterns for the simulated maps (i.e. alternation of flooded and dry pixels, caused by unrealistic elevation differences between adjacent pixels), but also to errors in the flood extent detected from satellite images. Moreover, the presence of several isolated small flooded areas in the detected flood maps suggests that the image might have been taken after the flood peak, thus underestimating the maximum flood extent. Finally, the presence of embankments not simulated by the model may contribute to reduce the overall skill.

### 3.3 | Comparison against official flood hazard maps

#### 3.3.1 | Comparison of the 500 years return period

Another approach for the validation of our method is to carry out a comparison with existing high-resolution flood hazard maps (Alfieri et al., 2013; Sampson et al., 2015; Winsemius et al., 2016). The simulated ICTP2H flood hazard maps, hereafter referred to as 'ICTP2H maps', are tested against the official hazard AdbPo flood maps produced by the Po river basin

authority. According to the available technical documentation (Autorità di bacino del fiume Po, 2012), the flood hazard maps related to the main river networks were calculated using 1D hydraulic models, integrated by 2D simulations in specific areas of interest (e.g. near bridges or hydraulic structures). All simulations were based on surveyed topography and river bathymetry. The delineation of flood-prone areas outside of main river embankments were derived using GIS interpolation and considering terrain altimetry and geomorphologic features.

In addition, we compare the ICTP2H maps with the flood hazard maps produced by the Joint Research Centre of the European Commission (JRC), which are freely available online and are based on streamflow data from the European Flood Awareness System (EFAS, Demeritt, Nobert, Cloke, & Pappenberger, 2013) at a spatial resolution of 3" (Dottori et al., 2016a, 2016b, 2016c). A detailed description of the JRC modelling framework is reported by Alfieri et al. (2014) and Alfieri et al. (2015). While the JRC and our framework share a number of methods (e.g. the construction of flood hydrographs and flood maps), they use different models and datasets and diverge in other modelling solutions. For instance, the conveyance of the river channel is derived here using the 'digging method' (described in Section 2.4.2), while the JRC flood maps account for this effect by removing the 2-year return period discharge.

To calculate the indices, we focus on two smaller portions of the domain, shown in Figure 5: Box 1 centred on the main river, and Box 2 centred on a tributary region. In Box 1, we removed flooded areas originating from river sections with an upstream area smaller than 500 km<sup>2</sup>, since they are not simulated and therefore not included in the JRC maps. Box 2 was left unmodified to evaluate the ability of the new approach in modelling floods originated by smaller rivers with upstream areas smaller than 500 km<sup>2</sup>.

The comparison against official hazard maps must take into consideration the complex configuration of the Po floodplain. The main stem of the Po River is characterised by a stable main channel and a floodplain (overall width varying between 200 m and 5 km) confined by two continuous main embankments, designed to protect the rest of the Po floodplain for flood events with return periods up to 200 years. In addition, some areas within the river channel and main embankment are protected against frequent flooding by a system of minor dykes with different design standards. As such, the simulation of flood dynamics for events with  $R_p$  equal or below 200 years would require a detailed representation of the embankment system (Wing et al., 2019). However, neither the JRC nor ICTP2H maps consider the embankment system, since they are not represented in the DEMs

TABLE 1 Evaluation of the ICTP2H flooded extent against observation for the case studies shown in Figure 7

	Hit rate	False alarm	Critical success
Case (a)	0.82	0.31	0.62
Case (b)	0.55	0.65	0.28

used in the two studies. For this reason, we decided to limit the numerical comparison only against the AdbPo maps for the 500-year return period ( $F_o$ ) shown in Figure 8. Indices (Equations 4–6) were calculated for the two boxes both for the ICTP2H and JRC maps ( $F_m$ ) and are reported in Table 2.

As can be seen, in Box 1 the ICTP2H maps provide fairly good results for the 500 years return period, with a  $H_R$  of 0.76, a  $C_S$  index of 0.67 and a very low false alarm value (0.12). The JRC maps have slightly higher scores, with a  $H_R$  of 0.83, a  $C_S$  of 0.73 but also higher false alarm  $F_A$  of 0.15. Notably, the performances of both models are above the CS threshold of 0.65 proposed by Fleischmann,

Paiva, and Collischonn (2019) to identify large-scale maps with local relevance (e.g. comparable to local-scale detailed studies). The different skills of the two approaches may originate from a difference in overall flood volumes (smaller in ICTP2H simulations, larger in JRC simulations). This would be consistent with the higher HR and FAR rates of the JRC maps, which indicate a larger flood extent. The difference in flood volumes might derive from the different hydrological models and climatological data used to prepare input hydrographs. In addition, the channel digging approach might produce a higher conveyance capacity with respect to the JRC simulations (where overall flood discharge is reduced by the

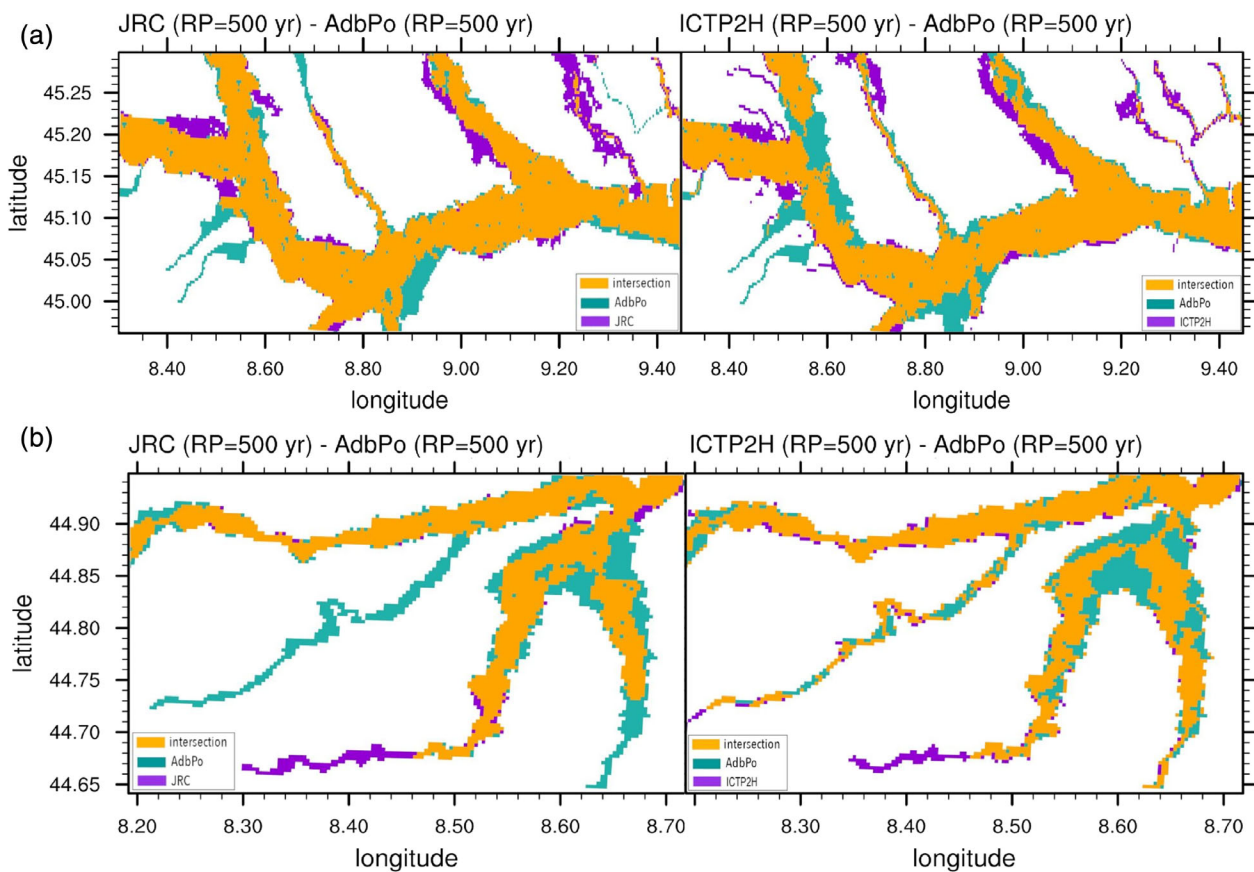


**FIGURE 8** ICTP2H and JRC flood hazard maps for the 500 years return period compared to AdbPo flood hazard maps. Box 1 (2) results are shown in the upper (lower) panels

**TABLE 2** Evaluation of the ICTP2H and JRC flooded extent against official flood hazard maps (Adbpo) for the return period of 500 years for the two boxes illustrated in Figure 5

		Hit rate	False alarm	Critical success
Box 1	JRC	0.83	0.15	0.73
	ICTP2H	0.76	0.12	0.67
Box 2	JRC	0.62	0.08	0.57
	ICTP2H	0.69	0.04	0.63



1-in-2-year discharge value), thus resulting in lower floodwater volumes. Finally, the different DEMs may generate further differences between the JRC and ICTP2H flood extent.

In Box 2, the ICTP2H maps show a better performance compared to the JRC and they present higher  $H_R$  and  $C_S$  (0.69 and 0.63 against 0.62 and 0.57, respectively) and a lower  $F_A$  index (0.04 respect to 0.08). These results highlight two aspects of the new approach. The first being the ability of the method to be applicable to any catchment independently from the size and therefore in this case to be able to simulate floods generated by rivers with an upstream area smaller than 500 km<sup>2</sup>. The second being that by not having any constraints on the basin resolution it can be portable in any domain where there are for example only small catchments and at any resolution.

### 3.3.2 | Comparison of the smaller return periods

All the cases considered so far include flood events with high return periods, where the contribution of the

estimated channel depths to the flood maps is difficult to separate from other model components. In order to better investigate the behaviour of the channel digging method, here we analyse the results of a comparison of the ICTP2H and JRC maps against official maps for flood events with return periods of 20–50 years, and 100–200 years (Box 1 in Figure 9 and Box 2 in Figure 10). As mentioned in Section 3.3.1, in both official maps the flood extent is limited to a small area enclosed by the main embankments of the Po river main stem and major tributaries, with some differences between the 20–50 and 100–200 maps due to the minor dikes. Given that neither the main embankments nor the minor dykes are included in ICTP2H and JRC flood models, the skill of both simulated maps is low ( $C_S$  scores are below 0.4 for the Box 1 and around 0.5 for the Box 2), but some of the observed differences are worth mentioning.

In both Box 1 and Box 2, the JRC maps overestimate the flood extent for return periods lower than 200 years, as the input elevation data of the DEM are not altered. Overestimation also occurs in the ICTP2H maps over some parts of the main river, as visible in the two real case studies described in Section 3.2. In the tributary

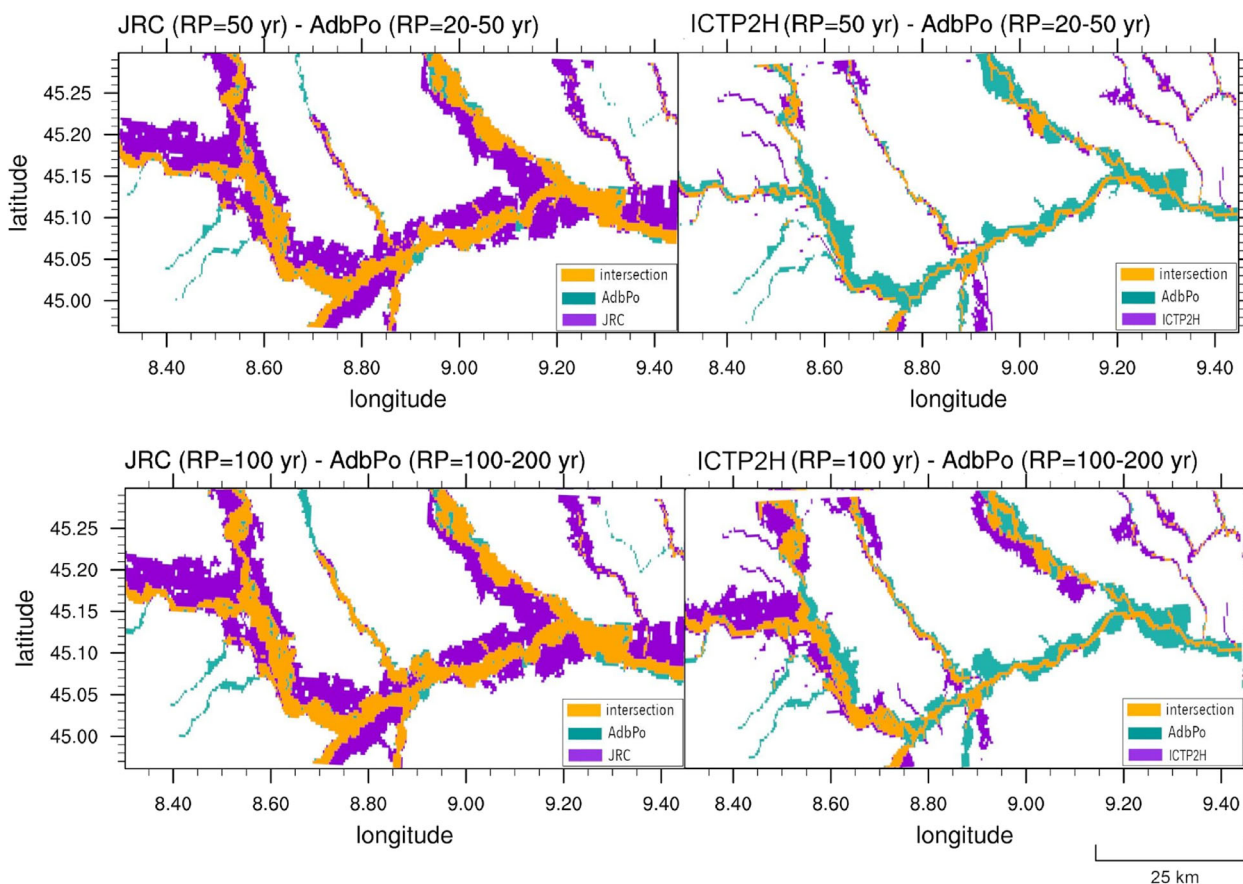
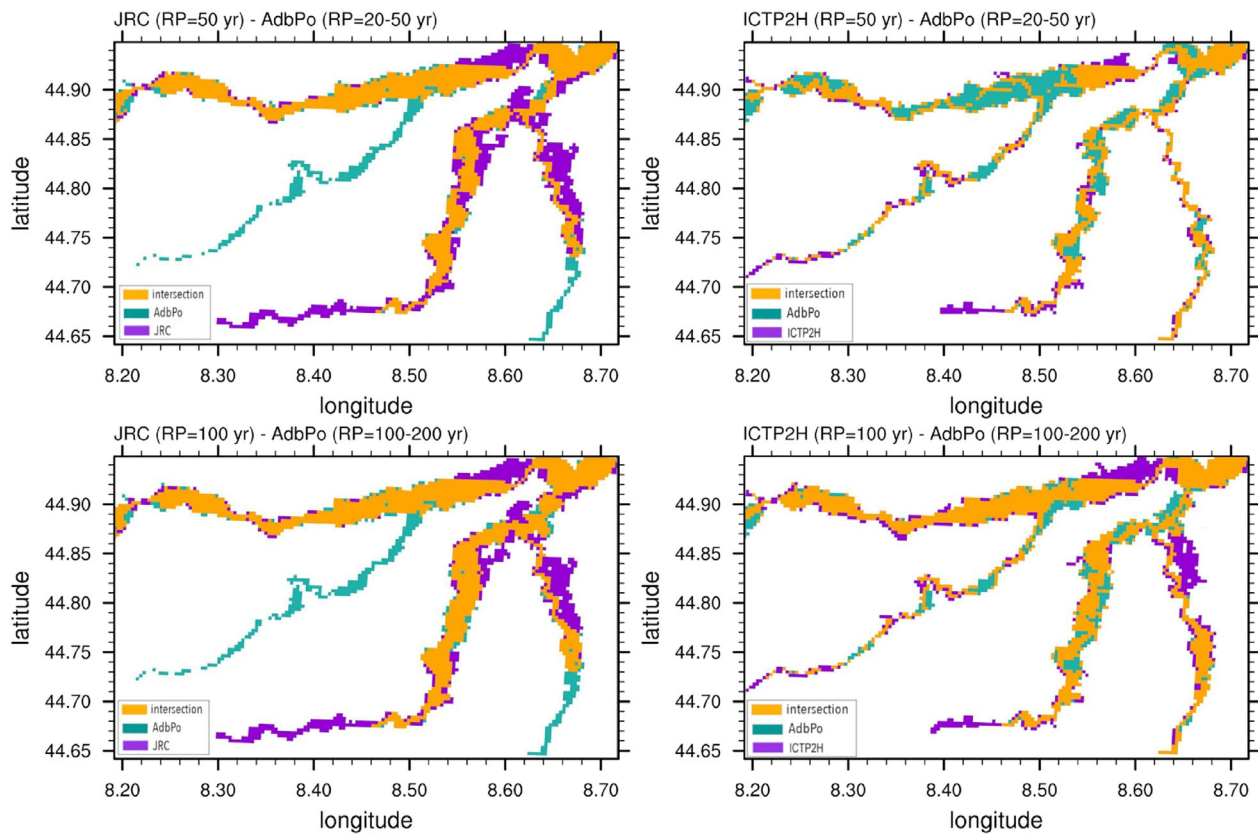


FIGURE 9 Box 1 ICTP2H and JRC flood hazard maps for the 50 and 100 years return period compared to AdbPo flood hazard maps for 20–50 and 100–200 years return periods





**FIGURE 10** Box 2 ICTP2H and JRC flood hazard maps for the 50 and 100 years return period compared to AdbPo flood hazard maps for 20–50 and 100–200 years return periods

region (Figure 10), the ICTP2H maps are well able to simulate smaller river floods also for return periods below 200 years, with reduced false alarm areas. These results confirm that the channel digging method increases the sensitivity of the flood extent maps to the return period.

However, underestimation occurs in a few reaches such as some sections of the Po main stem protected by minor dykes. This is probably an effect of the noise in the SRTM elevation values, which produces a river longitudinal profile with spikes and pits. Since the digging procedure is designed to iteratively lower the elevation of all river bed pixels until overflowing is prevented in nearby sections, this may produce considerable river bed depths where river bed pixels already have a low elevation. This result suggests that additional work is needed to refine the methodology.

A possible solution to reduce the elevation noise could be the use of recent elevation datasets such as MERIT HYDRO (Yamazaki et al., 2019), where elevations of river beds are smoothed to better reproduce the drainage network and river hydrology. In addition, having information on river bed conveyance capacity (or possibly flood extent data for low-return period flood

events) would allow us to evaluate the digging method, however such information is currently not publicly available for the Po river basins or in other river basins in Italy. Overall, these results confirm that the inclusion of a river channel network is necessary to guarantee acceptable results in the simulation of flood depths and extent for all return periods (Neal et al., 2012).

## 4 | CONCLUSIONS

In this article, we investigate the feasibility of producing high-resolution flood maps for Italy using a combined hydrological-hydraulic modelling framework, showing the illustrative example of the Po river basin and taking advantage of the most updated meteorological and hydrological measurements and surface elevation data. To improve the modelling of flood processes we use an innovative approach which reshapes the digital elevation models by a ‘digging’ procedure that assumes that floods should never occur for discharges associated with a return period of 1.5 years, as it represents the conveyance capacity of the river channel. Although we are aware that for example most of the river networks in Europe have

an average protection level of 100y  $R_P$  (Paprotny, Morales-Nápoles, & Jonkman, 2017; Rojas, Feyen, & Watkiss, 2013), the main purpose of this method is: (i) to allow application also in those regions where there is no available information about river natural banks; and (ii) to be of use in a climate projection mode, estimating possible changes of any flood return period for each river segment.

To this aim a 2-dimensional hydraulic model is used to simulate the propagation of water across the HydroSHEDS DEM, which was processed to yield an estimate of bankfull discharge. The evaluation of flood maps produced with this method was carried out on two real case flood images and through existing official flood maps from the Po river basin authority (Adbpo) over two portions of the domain centred, respectively, on the main river and on a tributary region. We also compared our results with an additional dataset of European flood maps produced at the JRC using a previous version of the hydraulic model. Given the complex embankment system protecting the Po river floodplains, the assessment against Adbpo flood maps was carried out only for the 500y  $R_P$  and this showed a good spatial agreement between the ICTP2H and Adbpo flood area extent. Moreover, the new developed method is shown to have an added value compared to the JRC method particularly evident on small basins (drained area  $<500 \text{ km}^2$ ); being this a quite important characteristic when higher resolutions of any area drained by small basins wants to be explored.

For this reason, the ICTP2H flood maps include a larger extent of the river network compared to the JRC maps thanks to the use of more accurate national-scale datasets which allows us to model the flow regime of minor river networks. We also showed how the DEM-resampling method improves the sensitivity of the ICTP2H flood extent maps to the return period compared to the JRC maps, although some underestimation occurs in few reaches. This aspect will be further investigated by means of a combined use of observed data of river bed depth and width (Andreadis et al., 2013; Yamazaki et al., 2014), and which will constitute a more realistic representation of the geometry of the river channel. In addition the use of the more recent DEM MERIT HYDRO (Yamazaki et al., 2019), will allow a better representation of the elevation. The reason for the choice of the upper Po river basin in our study was due to the relatively high density of data available, however the method was developed for application to larger domains, such as the Italian or European regions. In fact, the method can be especially useful for regions around the world where most of the basins are ungauged and there is no information available on the protection levels.

Future study entails the application of our method to larger regions using information from regional climate model downscaled scenario simulations as input to the hydrological and hydraulic models. This will provide useful information for stakeholders and policy makers on how the present day flood return period may change in future climate scenarios, information that will be crucial for adaptation and mitigation strategy development such as, for example, the construction of new river bank protection.

## ACKNOWLEDGEMENTS

The authors gratefully acknowledge the financial support of the Allianz Insurance Company for the realization of this project and Dr. Marco Verdecchia from the University of L'Aquila for providing the discharges observational datasets. The research reported in this study was supported by OGS and CINECA under HPC-TRES program award number 2020-12.

## CONFLICT OF INTEREST

The authors declare no conflict of interest.

## AUTHOR CONTRIBUTIONS

Rita Nogherotto, Adriano Fantini, Francesca Raffaele and Erika Coppola conceived and planned the experiments. Rita Nogherotto, Adriano Fantini, Francesca Raffaele and Erika Coppola planned and carried out the simulations. Fabio Di Sante and Francesco Dottori designed the model and the computational framework. Rita Nogherotto, Adriano Fantini, Francesca Raffaele, Erika Coppola and Francesco Dottori contributed to the interpretation of the results. Rita Nogherotto took the lead in writing the manuscript. All authors provided critical feedback and helped shape the research, analysis and manuscript.

## DATA AVAILABILITY STATEMENT

Data sharing is not applicable to this article as no new data were created or analyzed in this study.

## ORCID

Rita Nogherotto  <https://orcid.org/0000-0003-1718-542X>

## REFERENCES

- Albano, R., Mancusi, L., & Abbate, A. (2017). Improving flood risk analysis for effectively supporting the implementation of flood risk management plans: The case study of "Serio" valley. *Environmental Science & Policy*, 75, 158–172.
- Alfieri, L., Burek, P., Dutra, E., Krzeminski, B., Muraro, D., Thielen, J., & Pappenberger, F. (2013). GloFAS-global ensemble streamflow forecasting and flood early warning. *Hydrology and Earth System Sciences*, 17, 1161–1175.
- Alfieri, L., Burek, P., Feyen, L., & Forzieri, G. (2015). Global warming increases the frequency of river floods in Europe. *Hydrology and Earth System Sciences*, 19, 2247–2260.

- Alfieri, L., Salamon, P., Bianchi, A., Neal, J., Bates, P., & Feyen, L. (2014). Advances in panEuropean flood hazard mapping. *Hydrological Processes*, 28, 4067–4077.
- Amadio, M., Mysiak, J., Pecora, S., & Agnetti, A. (2013). Looking forward from the past: Assessing the potential flood hazard and damage in polesine region by revisiting the 1950. *Flood Event*.
- Andreadis, K., Schumann, G., & Pavelsky, T. (2013). A simple global river bankfull width and depth database. *Water Resources Research*, 49, 7164–7168.
- Autorita' di bacino del fiume Po, Progetto di Variante al PAI: mappe della pericolosità e del rischio di alluvione (in Italian), <https://pianoalluvioni.adbpo.it/progetto-esecutivo-delleattivita/>, 2012.
- Balz, T., & Stilla, U. (2009). Hybrid GPU-based single-and double-bounce SAR simulation. *IEEE Transactions on Geoscience and Remote Sensing*, 47, 3519–3529.
- Bárdossy, A. (2007). Calibration of hydrological model parameters for ungauged catchments. *Hydrology and Earth System Sciences Discussions*, 11, 703–710.
- Bates, P., & de Roo, A. (2000). A simple raster-based model for flood inundation simulation. *Journal of Hydrology*, 236, 54–77.
- Bates, P., Horritt, M., & Fewtrell, T. (2010). A simple inertial formulation of the shallow water equations for efficient two-dimensional flood inundation modelling. *Journal of Hydrology*, 387, 33–45.
- Bianco, L., Tomassetti, B., Coppola, E., Fracassi, A., Verdecchia, M., & Visconti, G. (2006). Thermally driven circulation in a region of complex topography: Comparison of windprofiling radar measurements and MM5 numerical predictions. *Annales Geophysicae*, 24(6), 1537–1549. <https://doi.org/10.5194/angeo-24-1537-2006>
- Brandimarte, L., & Di Baldassarre, G. (2012). Uncertainty in design flood profiles derived by hydraulic modelling. *Hydrology Research*, 43, 753–761.
- Castellarin, A., Domeneghetti, A., & Brath, A. (2011). Identifying robust large-scale flood risk mitigation strategies: A quasi-2D hydraulic model as a tool for the Po river, physics and chemistry of the earth. *Parts A/B/C*, 36, 299–308.
- Copernicus Land Monitoring Service, Corine Land Cover, <http://land.copernicus.eu/paneurpean/corine-land-cover>, 2020.
- Coppola, E., Tomassetti, B., Mariotti, L., Verdecchia, M., & Visconti, G. (2007). Cellular automata algorithms for drainage network extraction and rainfall data assimilation. *Hydrological Sciences Journal*, 52, 579–592.
- Coppola, E., Verdecchia, M., Giorgi, F., Colaiuda, V., Tomassetti, B., & Lombardi, A. (2014). Changing hydrological conditions in the Po basin under global warming. *Science of the Total Environment*, 493, 1183–1196.
- Covello, F., Battazza, F., Coletta, A., Lopinto, E., Fiorentino, C., Pietranera, L., Valentini, G., & Zoffoli, S. (2010). COSMO-SkyMed an existing opportunity for observing the earth. *Journal of Geodynamics*, 49, 171–180.
- Demeritt, D., Nobert, S., Cloke, H. L., & Pappenberger, F. (2013). The European flood alert system and the communication, perception, and use of ensemble predictions for operational flood risk management. *Hydrological Processes*, 27, 147–157.
- di Baldassarre, G., Schumann, G., & Bates, P. (2009). Near real time satellite imagery to support and verify timely flood modelling. *Hydrological Processes: An International Journal*, 23, 799–803.
- Di Salvo, C., Ciotoli, G., Pennica, F., & Cavinato, G. P. (2017). Pluvial flood hazard in the city of Rome (Italy). *Journal of Maps*, 13, 545–553.
- Dottori, F., Alfieri, L., Bianchi, A., Skoien, J., & Salamon, P. (2021). A new dataset of river flood hazard maps for Europe and the Mediterranean Basin region. *Earth System Science Data Discussions*, 1–35.
- Dottori, F., Alfieri, L., Salamon, P., Bianchi, A., Feyen, L., and Lorini, V. Flood hazard map for Europe, 100-year return period, European Commission, Joint Research Centre (JRC) [Dataset]. <http://data.europa.eu/89h/jrc-floods-floodmapeurop100y-tif>, 2016a.
- Dottori, F., Alfieri, L., Salamon, P., Bianchi, A., Feyen, L., and Lorini, V. Flood hazard map for Europe, 50-year return period, European Commission, Joint Research Centre (JRC)[Dataset] <http://data.europa.eu/89h/jrc-floods-floodmapeurop50y-tif>, 2016b.
- Dottori, F., Alfieri, L., Salamon, P., Bianchi, A., Feyen, L., and Lorini, V., Flood hazard map for Europe, 500-year return period, European Commission, Joint Research Centre (JRC) [Dataset]. <http://data.europa.eu/89h/jrc-floods-floodmapeurop500y-tif>, 2016c.
- Dottori, F., Salamon, P., Bianchi, A., Alfieri, L., Hirpa, F., & Feyen, L. (2016). Development and evaluation of a framework for global flood hazard mapping. *Advances in Water Resources*, 94, 87–102.
- Dottori, F., & Todini, E. (2011). Developments of a flood inundation model based on the cellular automata approach: Testing different methods to improve model performance. *Physics and Chemistry of the Earth Parts A/B/C*, 36, 266–280.
- European Commission. (2007). Directive 2007/60/EC of the European Parliament and of the council of 23 October 2007 on the assessment and management of flood risks. *Journal of the European Union*, L, 288, 27–34.
- EWA: European Water Archive (EWA) of EURO-FRIEND-Water. <https://www.bafg.de/GRDC/EN/04spcldtbss/42EWA/ewanode.html>, 2014.
- Fantini, A.: Climate change impact on flood hazard over Italy, Ph. D. thesis, University of Trieste, 2019.
- Fantini, A., Di Sante, F., Coppola, E., Verdecchia, M., and Giuliani, G.: GRIPHO: a gridded high-resolution hourly precipitation dataset over Italy, in preparation, 2021.
- Farr, T., Rosen, P., Caro, E., Crippen, R., Duren, R., Hensley, S., Kobrick, M., Paller, M., Rodriguez, E., Roth, L., Seal, D., Shaffer, S., Shimada, J., Umland, J., Werner, M., Oskin, M., Burbank, D., & Alsdorf, D. (2007). The shuttle radar topography mission. *Reviews of Geophysics*, 45, 1–3.
- Fleischmann, A., Paiva, R., & Collischonn, W. (2019). Can regional to continental river hydrodynamic models be locally relevant? A cross-scale comparison. *Journal of Hydrology X*, 3, 100027.
- Grell, G., Dudhia, J., and Stauffer, D.: A description of the fifth-generation Penn State/NCAR mesoscale model (MM5), Technical Report, doi:<https://doi.org/10.5065/D60Z716B>, 1994.
- Harman, C., Stewardson, M., & DeRose, R. (2008). Variability and uncertainty in reach bankfull hydraulic geometry. *Journal of Hydrology*, 351, 13–25.
- Hirt, C., Filmer, M., & Featherstone, W. (2010). Comparison and validation of the recent freely available ASTER-GDEM ver1, SRTM ver4. 1 and GEODATA DEM-9S ver3 digital elevation



- models over Australia. *Australian Journal of Earth Sciences*, 57, 337–347.
- Horritt, M., & Bates, P. (2002). Evaluation of 1D and 2D numerical models for predicting river flood inundation. *Journal of Hydrology*, 268, 87–99.
- ISPRA, P. M. E. Italian National Institute for Environmental Protection and Research, 2017.
- Istituto di Ricerca per la Protezione Idrologica and Consiglio Nazionale delle Ricerche: Polaris: Rapporto Periodico 2017 sul Rischio posto alla Popolazione italiana da Frane e Inondazioni, Tech. rep. IRPI/CNR. <http://polaris.irpi.cnr.it/wpcontent/uploads/report-2017.pdf>, 2018.
- Jenson, S. K., & Domingue, J. O. (1988). Extracting topographic structure from digital elevation data for geographic information system analysis. *Photogrammetric Engineering and Remote Sensing*, 54, 1593–1600.
- Jing, C., Shortridge, A., Lin, S., & Wu, J. (2014). Comparison and validation of SRTM and ASTER GDEM for a subtropical landscape in southeastern China. *International Journal of Digital Earth*, 7, 969–992.
- Khan, S., Hong, Y., Wang, J., Yilmaz, K., Gourley, J., Adler, R., Brakenridge, G., Policelli, F., Habib, S., & Irwin, D. (2011). Satellite remote sensing and hydrologic modeling for flood inundation mapping in Lake Victoria basin: Implications for hydrologic prediction in ungauged basins. *IEEE Transactions on Geoscience and Remote Sensing*, 49, 85–95.
- Lehner, B., Verdin, K., and Jarvis, A.: *HydroSHEDS technical documentation*, version 1.0, World Wildlife Fund US, pp. 1–27, 2006.
- Lehner, B., Verdin, K., & Jarvis, A. (2008). New global hydrography derived from spaceborne elevation data, Eos. *Transactions American Geophysical Union*, 89, 93–94.
- Lehner, B., Verdin, K., and Jarvis, A.: *HydroSHEDS Technical Documentation Version 1.2*, EOS Transactions, 2013.
- Leopold, L. (1994). *A view of the river*. Harvard University Press.
- Lighthill, M., & Whitham, G. (1955). On kinematic waves. I. Flood movement in long Rivers, proceedings of the Royal Society a: Mathematical. *Physical and Engineering Sciences*, 229(1178), 281–316. <https://doi.org/10.1098/rspa.1955.0088>
- Maione, U., Mignosa, P., & Tomirotti, M. (2003). Regional estimation model of synthetic design hydrographs. *International Journal of River Basin Management*, 12, 151–163.
- Marchesini, I., Rossi, M., Salvati, P., Donnini, M., Sterlacchini, S., & Guzzetti, F. (2016). Delineating flood prone areas using a statistical approach. *PeerJ Preprints*, 4, e1937v1.
- Marchi, L., Borga, M., Preciso, E., & Gaume, E. (2010). Characterisation of selected extreme flash floods in Europe and implications for flood risk management. *Journal of Hydrology*, 394, 118–133.
- Martz, L. W., & Garbrecht, J. (1992). Numerical definition of drainage network and subcatchment areas from digital elevation models. *Computers & Geosciences*, 18, 747–761.
- Masoero, A., Claps, P., Asselman, N. E., Mosselman, E., & Di Baldassarre, G. (2013). Reconstruction and analysis of the Po River inundation of 1951. *Hydrological Processes*, 27, 1341–1348.
- Montanari, A. (2012). Hydrology of the Po River: Looking for changing patterns in river discharge. *Hydrology and Earth System Sciences*, 16, 3739–3747.
- Morelli, S., Battistini, A., & Catani, F. (2014). Rapid assessment of flood susceptibility in urbanized rivers using digital terrain data: Application to the Arno river case study (Firenze, northern Italy). *Applied Geography*, 54, 35–53.
- Neal, J., Schumann, G., & Bates, P. (2012). A subgrid channel model for simulating river hydraulics and floodplain inundation over large and data sparse areas. *Water Resources Research*, 48(11), 1–16.
- Norbiato, D., Borga, M., Sangati, M., & Zanon, F. (2007). Regional frequency analysis of extreme precipitation in the eastern Italian Alps and the august 29, 2003 flash flood. *Journal of Hydrology*, 345, 149–166.
- Pappenberger, F., Dutra, E., Wetterhall, F., & Cloke, H. (2012). Deriving global flood hazard maps of fluvial floods through a physical model cascade. *Hydrology and Earth System Sciences*, 16, 4143–4156.
- Paprotny, D., & Morales-Nápoles, O. (2017). Estimating extreme river discharges in Europe through a Bayesian network. *Hydrology & Earth System Sciences*, 21, 2615–2636.
- Paprotny, D., Morales-Nápoles, O., & Jonkman, S. N. (2017). Efficient pan-European river flood hazard modelling through a combination of statistical and physical models. *Natural Hazards and Earth System Sciences*, 17, 1267–1283.
- Parsons, J. A., & Fonstad, M. A. (2007). A cellular automata model of surface water flow. *Hydrological Processes: An International Journal*, 21, 2189–2195.
- Pulvirenti, L., Pierdicca, N., & Chini, M. (2010). Analysis of Cosmo-SkyMed observations of the 2008 flood in Myanmar. *Italian Journal of Remote Sensing*, 42, 79–90.
- Rabus, B., Eineder, M., Roth, A., & Bamler, R. (2003). The shuttle radar topography mission: A new class of digital elevation models acquired by spaceborne radar. *ISPRS Journal of Photogrammetry and Remote Sensing*, 57, 241–262.
- Rojas, R., Feyen, L., Dosio, A., & Bavera, D. (2011). Improving pan-European hydrological simulation of extreme events through statistical bias correction of RCM-driven climate simulations. *Hydrology & Earth System Sciences*, 15, 2599–2620.
- Rojas, R., Feyen, L., & Watkiss, P. (2013). Climate change and river floods in the European Union: Socio-economic consequences and the costs and benefits of adaptation. *Global Environmental Change*, 23, 1737–1751.
- Rudari, R., Silvestro, F., Campo, L., Rebora, N., Boni, G., & Herold, C. (2015). *Improvement of the global food model for the GAR 2015*, United Nations Office for disaster risk reduction (UNISDR), Centro Internazionale in Monitoraggio Ambientale (CIIMA) (p. 69). UNEP GRIDArendal (GRID-Arendal).
- Salvati, P., Bianchi, C., Rossi, M., & Guzzetti, F. (2010). Societal landslide and flood risk in Italy. *Natural Hazards & Earth System Sciences*, 10, 465–483.
- Sampson, C., Smith, A., Bates, P., Neal, J., Alfieri, L., & Freer, J. (2015). A high-resolution global flood hazard model. *Water Resources Research*, 51, 7358–7381.
- Santo, A., Di Crescenzo, G., Del Prete, S., & Di Iorio, L. (2012). The Ischia Island flash flood of November 2009 (Italy): Phenomenon analysis and flood hazard. *Physics and Chemistry of the Earth, Parts A/B/C*, 49, 3–17.
- Scussolini, P., Aerts, J. C. J. H., Jongman, B., Bouwer, L. M., Winsemius, H. C., de Moel, H., & Ward, P. J. (2016). FLOPROS: An evolving global database of flood protection standards. *Natural Hazards & Earth System Sciences*, 16, 1049–1061.



- Sole, A., Giosa, L., Nol'e, L., Medina, V., & Bateman, A. (2008). Flood risk modelling with LiDAR technology. *Flood Recovery, Innovation and Response*, 118, 27–36.
- Te Linde, A., Bubeck, P., Dekkers, J., De Moel, H., & Aerts, J. (2011). Future flood risk estimates along the river Rhine. *Natural Hazards and Earth System Sciences*, 11, 459–473.
- Thornthwaite, C. W. and Mather, J. R.: Instructions and tables for computing potential evapotranspiration and water balance, 1957.
- Todini, E. (1996). The ARNO rainfall: Runoff model. *Journal of Hydrology*, 175, 339–382.
- Tomassetti, B., Coppola, E., Verdecchia, M., & Visconti, G. (2005a). Coupling a distributed grid based hydrological model and MM5 meteorological model for flooding alert mapping. *Advances in Geosciences*, 1, 59–63. <https://doi.org/10.5194/adgeo-2-59-2005>
- Tribe, A. (1992). Automated recognition of valley lines and drainage networks from grid digital elevation models: A review and a new method. *Journal of Hydrology*, 139, 263–293.
- Verdecchia, M., Coppola, E., Faccani, C., Ferretti, R., Memmo, A., Montopoli, M., Rivolta, G., Paolucci, T., Picciotti, E., Santacasa, A., Tomassetti, B., Visconti, G., & Marzano, F. (2008). Flood forecast in complex orography coupling distributed hydro-meteorological models and in-situ and remote sensing data. *Meteorology and Atmospheric Physics*, 101(3), 267–285. <https://doi.org/10.1007/s00703007-0278-z>
- Verdecchia, M., Coppola, E., Tomassetti, B., & Visconti, G. (2009). Cetemps hydrological model (CHyM), a distributed grid-based model assimilating different rainfall data sources. In *Hydrological modelling and the water cycle* (pp. 165–201). Springer.
- Wing, O. E., Bates, P. D., Neal, J. C., Sampson, C. C., Smith, A. M., Quinn, N., Shustikova, I., Domeneghetti, A., Gilles, D. W., Goska, R., & Krajewski, W. F. (2019). A new automated method for improved flood defense representation in large-scale hydraulic models. *Water Resources Research*, 55, 11007–11034.
- Wing, O. E., Bates, P. D., Sampson, C. C., Smith, A. M., Johnson, K. A., & Erickson, T. A. (2017). Validation of a 30 m resolution flood hazard model of the conterminous United States. *Water Resources Research*, 53, 7968–7986.
- Winsemius, H., Aerts, J., van Beek, L., Bierkens, M., Bouwman, A., Jongman, B., Kwadijk, J., Ligtoet, W., Lucas, P., van Vuuren, D., & Ward, P. J. (2016). Global drivers of future river flood risk. *Nature Climate Change*, 6, 381–385.
- Yamazaki, D., Ikeshima, D., Sosa, J., Bates, P. D., Allen, G. H., & Pavelsky, T. M. (2019). MERIT hydro: A high-resolution global hydrography map based on latest topography dataset. *Water Resources Research*, 55, 5053–5073.
- Yamazaki, D., O'Loughlin, F., Trigg, M. A., Miller, Z. F., Pavelsky, T. M., & Bates, P. D. (2014). Development of the global width database for large rivers. *Water Resources Research*, 50, 3467–3480.

**How to cite this article:** Nogherotto, R., Fantini, A., Raffaele, F., Di Sante, F., Dottori, F., Coppola, E., & Giorgi, F. (2022). A combined hydrological and hydraulic modelling approach for the flood hazard mapping of the Po river basin. *Journal of Flood Risk Management*, 15(1), e12755. <https://doi.org/10.1111/jfr3.12755>